JBIR-22, An Inhibitor for Protein−Protein Interaction of the Homodimer of Proteasome Assembly Factor 3

Miho Izumikawa,[†,⊥] Junko Hashimoto,[†,⊥] Takatsugu Hirokawa,[‡] Satoshi Sugimoto,[§] Taira Kato,[§] Motoki Takagi,*[,†] and Kazuo Shin-ya*[,‖]

Biomedicinal Information Research Center (BIRC), Japan Biological Informatics Consortium (JBIC), 2-4-7 Aomi, Koto-ku, Tokyo 135-0064, Japan, Computational Biology Research Center (CBRC), National Institute of Advanced Industrial Science and Technology (AIST), 2-4-7 Aomi, Koto-ku, Tokyo 135-0064, Japan, Bioresource Laboratories, Mercian Corporation, 1808 Nakaizumi, Iwata, Shizuoka 438-0078, Japan, Biomedicinal Information Research Center (BIRC), National Institute of Advanced Industrial Science and Technology (AIST), 2-4-7 Aomi, Koto-ku, Tokyo 135-0064, Japan

Proteasome assembling chaperone (PAC) 3 acts as a homodimer and plays an important role in proteasome formation. We screened JBIR-22 (**1**) as an inhibitor for protein−protein interaction (PPI) of PAC3 homodimer from our natural product library using a protein fragment complementation assay (PCA) with monomeric Kusabira-Green fluorescent protein (mKG) in vitro and found that **1** exhibited potent inhibitory activity against PAC3 homodimerization. Compound **1** showed long-term cytotoxicity against the human cervical carcinoma cell line, HeLa. This is the first report of a PPI inhibitor for proteasome assembly factors.

Protein−protein interactions (PPIs) play key roles in all cellular processes and have been validated as relevant pharmaceutical targets using modern proteome analyses. Thus, screening of PPI regulators is a means to discover novel drugs. Regulation of a typical protein−protein interface with a small molecule is generally thought to be difficult because approximately 750−1,500 Å^2 of its surface area is buried on each side of the interface. However, because the subset of the interface that contributes to high affinity binding (the "hot spot") is often much smaller,[1,2] it may not be necessary for small compounds to cover the entire protein-binding surface. In fact, examples of small compounds that bind directly to the hot spot of the protein−protein interface, or bind at allosteric sites distal from the protein−protein interface, have been reported.[1] Therefore, we have attempted to screen inhibitors of several PPIs from our natural product library.

To facilitate the screening of PPI inhibitors, we have developed a high-throughput screening (HTS) system using an in vitro protein fragment complementation assay (PCA) with monomeric Kusabira-Green fluorescent protein (mKG).[3] It has been reported that in mammalian cells, when mKG splits into two inactive fragments fused to two target proteins, it fluoresces due to the interaction between the target proteins.[4,5] We improved this in vivo system to make it applicable to an in vitro system. In this revised system, the two split fragment-fused proteins, which are independently prepared using a wheat germ cell-free protein synthesis system, are simply mixed, and the fluorescence emitted due to mKG complementation formed by the target protein interaction is measured. This system is applicable to HTS in a 1536-well microplate format and is advantageous in that it is very simple to handle and does not require protein purification and refolding. Using this system, we have succeeded in obtaining PPI inhibitors from our natural product library that function as anticancer drugs against three targets.[3]

Proteasome assembling chaperone (PAC) 3 is an assembly factor of the 20S proteasome and is essential for proteasome activity.[6,7]

The proteasome regulates protein expression and function by ubiquitinated protein degradation; it also contributes to the clearance of abnormal and misfolded proteins in cells. Cancer cells, involved in continuous proliferation, require higher proteasome activity than do normal cells. Proteasome inhibition prevents degradation of proapoptotic factors, permitting activation of programmed cell death in neoplastic cells possessing antiapoptotic pathways. The proteasome inhibitor bortezomib has been approved as a clinical agent for relapsed multiple myeloma and mantle-cell lymphoma.[8] We screened inhibitors of PAC3 homodimerization from a natural product library that includes microbial metabolites, plant extracts, and marine natural products. To date, we have reported three compounds, screened from 123599 samples, as inhibitors of PAC3 homodimerization.[3] Among these inhibitors, JBIR-22 (**1**) showed more potent inhibitory activity (IC$_{50}$ = 0.2 μM) for PAC3 homodimerization than did the other two PPIs, T-cell factor-7 with β-catenin (IC$_{50}$ = 6 μM) and PAC1 with PAC2 (IC$_{50}$ = 6 μM).[3] Thus, **1** may be a potential proteasome inhibitor. However, the structure of **1** isolated from fungal metabolites has not been clarified. In this study, the structure elucidation of **1** isolated from a fungal culture revealed **1** to be a new equisetin analogue on the basis of extensive NMR and MS analyses. Furthermore, docking studies of **1** with the X-ray structure of PAC3 revealed that **1** may preferably bind to the interface of the PAC3-binding domain.

JBIR-22 (**1**) : R = H
JBIR-22 methyl ester (**2**): R = CH$_3$

Equisetin

* To whom correspondence should be addressed. For M.T.: phone, +81-3-3599-8304; fax, +81-3-3599-8494; E-mail, motoki-takagi@aist.go.jp. For K.S.: phone, +81-3-3599-8854; fax, +81-3-3599-8494; E-mail, k-shinya@aist.go.jp.
    † JBIC.
    ‡ CBRC, AIST.
    § Mercian Corporation.
    ‖ BIRC, AIST.
    ⊥ The authors M. Izumikawa and J. Hashimoto equally contributed to this work.
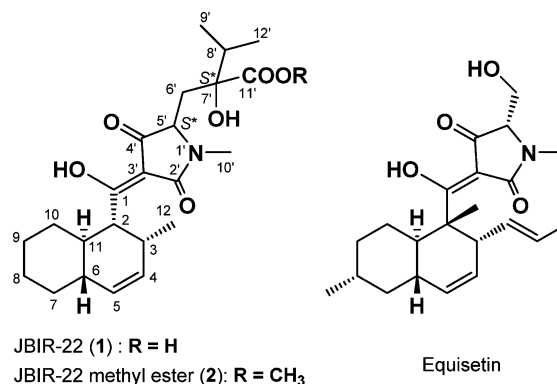
Results and Discussion

PPI inhibitors of the PAC3 homodimer were screened as potential anticancer drugs. As a result, we selected a sample of fungal

Table 1. ^{13}C (150 MHz) and ^{1}H (600 MHz) NMR Data of **1** in Acetone-d_6 and **2** in CDCl$_3$

		1		2	
no.	δ_C	δ_H (multiplicity, *J* in Hz)	δ_C	δ_H (multiplicity, *J* in Hz)
1	196.4		192.3	
2	51.0	3.90, dd (11.4, 5.7)	47.0	3.65, dd (1.6, 5.6)
3	32.2	2.64, ddq (7.1, 5.7, 2.3)	33.0	2.58, ddq (0.0, 5.6, 2.4)
4	133.6	5.53, dd (9.7, 2.3)	131.0	5.55, dq (9.7, 2.4)
5	131.1	5.30, d (9.7)	130.8	5.40, d (9.7)
6	43.4	1.68, ddd (12.3, 10.6, 4.8)	42.1	1.77, ddd (12.3, 10.2, 4.6)
7	34.3	1.69, ddd (9.4, 6.6, 4.8)	33.1	1.75, dddd (9.7, 6.2, 4.6, 1.2)
		1.03, ddt (12.3, 9.4, 6.5)		1.09, ddt (12.3, 9.7, 6.8)
8	27.6	1.65, m	26.4	1.73, m
		1.28, m		1.32, m
9	27.7	1.65, m	26.4	1.73, m
		1.28, m		1.32, m
10	31.0	1.97, dddd (12.9, 5.5, 4.3, 1.8)	30.0	1.80, dddd (12.4, 5.6, 4.7, 2.3)
		0.71, ddt (12.9, 11.7, 6.3)		0.88, ddt (12.4, 11.7, 6.1)
11	37.4	1.46, dddd (11.7, 11.4, 10.6, 4.3)	35.9	1.58, dddd (11.7, 11.6, 10.2, 4.7)
12	18.3	0.76, d (7.1)	16.3	0.96, d (7.0)
2′	174.6		173.4	
3′	101.9		101.3	
4′	196.1		195.9	
5′	63.3	3.36, dd (10.0, 1.2)	64.4	3.66, dd (9.5, 2.3)
6′	37.3	2.30, dd (13.6, 1.2)	34.4	2.33, dd (14.4, 2.3)
		1.60, dd (13.6, 10.0)		1.92, dd (14.4, 9.5)
7′	80.0		79.0	
8′	36.6	2.01, q (6.7)	36.8	2.05, q (7.0)
9′	18.7	0.91, d (6.7)	17.4	0.93, d (7.0)
10′	26.8	2.71, s	26.5	2.97, s
11′	180.9		176.0	
12′	16.8	0.89, d (6.7)	16.3	0.96, d (7.0)
7′-OH				5.18, br s
−COOMe			52.4	3.79, s

metabolite containing **1** from the 123599 samples in our natural product library using in vitro PCA with the mKG system. We then attempted to isolate the active compound from the sample.[3] We isolated the producer of **1**, *Verticillium* sp. f21794, from a soil sample via a new method[9] in which we applied the anthracycline antibiotic, daunomycin. The use of daunomycin in this method significantly prevents the growth of ordinary faster-growing fungi and, therefore, facilitates the selective isolation of rare slower-growing fungi. In fact, isolated *Verticillium* is a rare fungus, and reports of the bioactive compounds produced by *Verticillium* are limited. Nevertheless, we succeeded in isolating 4.8 mg of the new compound **1** from a culture (1.8 L) of *Verticillium* sp. f21794 by activity-guided separation.

We obtained **1** as a colorless amorphous solid and ascertained its molecular formula to be $C_{23}H_{33}NO_6$ (found: 420.2385 [M + H]$^+$, calculated: 420.2386) on the basis of HRESIMS analysis. The IR absorption band at 3243 cm^{-1} indicated the presence of a hydroxy group while the absorption band at 1658 cm^{-1} indicated the presence of α,β-unsaturated carbonyl and/or amide carbonyl groups. The structure of **1** was mainly determined by NMR analyses as follows.

We established the direct connectivity between each proton and carbon by the HSQC spectrum; the ^{13}C and ^{1}H NMR data for **1** are shown in Table 1. The DQF-COSY and constant time (CT)-HMBC spectra established three partial structures (Figure 1). The continuous correlations in $^{1}H-^{1}H$ couplings revealed the presence of a methyldecalin moiety. A $^{1}H-^{13}C$ long-range coupling from H-2 (δ_H 3.90) to an α,β-unsaturated carbonyl carbon C-1 (δ_C 196.4) revealed the substituted position of this carbonyl residue on the decalin moiety. An *N*-methyl proton H-10′ (δ_H 2.71) was $^{1}H-^{13}C$ long-range coupled to an amide carbonyl carbon C-2′ (δ_C 174.6) and a methine carbon C-5′ (δ_C 63.3), which was $^{1}H-^{1}H$ spin-coupled to methylene protons H-6′ (δ_H 2.30, 1.60). Long-range couplings from methyl proton doublets H-9′ (δ_H 0.91) and H-12′ (δ_H 0.89) to a methine carbon C-8′ (δ_C 36.6) and a quaternary carbon C-7′ (δ_C 80.0) established a 1-oxo-2-methylpropanoyl moiety. The $^{1}H-^{13}C$ long-range couplings from methylene protons

H-6′ and a methine proton H-8′ (δ_H 2.01) to a carboxylic carbonyl carbon C-11′ (δ_C 180.9), which was confirmed by the treatment of **1** with methyl iodide to form methyl ester **2**, established that the carboxylic acid residue was located at C-7′. Thus, the sequence from C-2′ to C-9′ was determined as shown in Figure 1. The $^{1}H-^{13}C$ long-range couplings from H-5′ and H-6′ to C-4′ (δ_C 196.1) revealed that C-4′ was connected to C-5′. By taking into consideration a remaining quaternary olefinic carbon C-3′ (δ_C 101.9) together with the typical ^{13}C NMR chemical shifts of C-4′ and the α,β-unsaturated carbonyl carbon C-1, the unit from C-1′ to C-5′ forms an α-acyltetramic acid moiety.[10] The UV spectrum of **1** also supports the presence of the tetramic acid functional group.[11] From the molecular formula of **1**, we established the planar structure of **1** as shown in Figure 1.

We inferred the relative configuration of the decalin moiety of **1**, as depicted in Figure 2a, from the analyses of $^{1}H-^{1}H$ coupling constants and a NOESY experiment. Large coupling constants between H-6/H-7a (δ_H 1.03), H-6/H-11, H-10a (δ_H 0.71)/H-11, and H-2/H-11 (*J* = 12.3, 10.6, 11.7, and 11.4 Hz, respectively) indicated that these protons were in diaxial orientations. The NOEs between H-11 and H-7a (δ_H 1.03) and the C-3 methyl protons confirmed
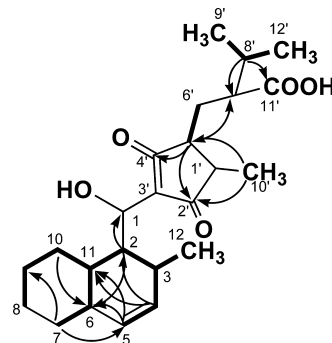
Figure 1. Key correlations in DQF-COSY (bold lines) and CT-HMBC (arrows) spectra of **1**.
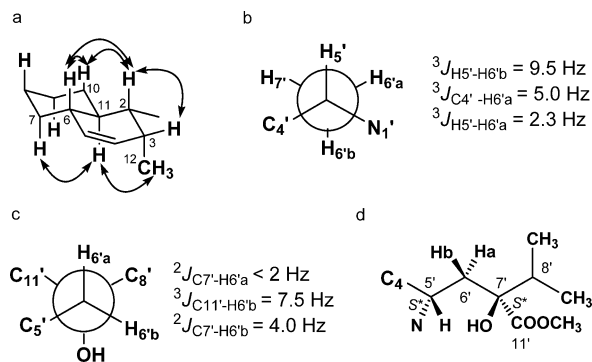
Figure 2. Configuration of **1** and **2**. (a) NOE correlations of the decalin moiety of **1**. (b) Relative configuration at C-5′ in **2**. (c) Relative configuration at C-7′ in **2**. (d) Relative configuration from C-5′ to C-7′ in **2**.

that these protons were cofacial. The NOEs among H-2, H-3, H-6, and H-10a (δ_H 0.71) also supported the relative configuration of the decalin moiety (Figure 2a).

To determine the relative configuration of the chain structure connected to the tetramic acid moiety, methylated derivative **2** was subjected to the *J*-based method.[12–15] In the *J*-resolved HMBC spectrum,[16] the large coupling constant ($^3J = 9.5$ Hz) between H-5′ and H-6′b (δ_H 1.92) indicated that these protons were anti-oriented. In addition, the large coupling constant ($^3J = 5.0$ Hz) indicated that H-6′a (δ_H 2.33) and C-4′ were also anti-oriented, as shown in Figure 2b. The small coupling constant ($^2J < 2$ Hz) revealed that H-6′a and the oxygen atom at C-7′ were anti-oriented, whereas the large coupling constant value ($^3J = 7.5$ Hz) between H-6′b and C-11′ suggested that H-6′b and C-11′ were anti-oriented (Figure 2c). Thus, the relative configurations at C-5′ and C-7′ were established as S* and S*, respectively (Figure 2d).

Compound **1** is similar to altersetin,[17] equisetin,[18,19] and trichosetin,[20] but it has a unique side chain. Altersetin and equisetin show antibacterial activity,[17] while trichosetin possesses inhibitory activities for root and shoot growth of plants.[21] Equisetin was also reported to inhibit HIV-1 integrase.[22] However, there has been no report of these compounds as regulators of proteasome activity. Therefore, we were interested in the mechanism by which **1** regulates the PAC3 molecule.

The crystal structure of the PAC3 homodimer has been previously reported.[23] Therefore, we performed docking studies of **1** onto the binding site of the PAC3 homodimer (Figure 3a) by employing the software 5.0 (SP mode). This model indicates that **1** can bind to the active site of PPI required for PAC3 homodimerization. Furthermore, the carboxylic group of **1** forms an ionic bond to the amino group of Lys65 in the interaction surface of the PAC3 homodimer, and the decalin moiety of **1** interacts with Leu96,

Leu33, and Phe28 of PAC3 through hydrophobic interaction (Figure 3b). We demonstrated that **1**, despite its small molecular weight (MW 419), can regulate the PPI of the PAC3 homodimer using the in vitro assay and the model of complex **1** and PAC3.

Because PAC3 promotes the formation of the 20S proteasome, which has a long half-life in mammalian cells, an inhibitor for PAC3 homodimerization would be expected to inhibit proteasome generation and induce a gradual decrease in proteasome activities. Hence, we evaluated the long-term cytotoxicity of **1** against cells of the human cervical carcinoma cell line, HeLa. Compound **1** showed cytotoxic activity with an IC$_{50}$ of 68 μM at 120 h but showed no effect at the same concentration at 48 h. The cytotoxic compounds, paclitaxel (tubulin inhibitor) and doxorubicin (DNA intercalater), exhibited cytotoxic activities with IC$_{50}$ values of 30 and 55 nM for 48 h, and 190 and 37 nM for 120 h, respectively. These results suggested that **1** may inhibit the generation of proteasome components.

We demonstrated that compound **1** specifically inhibits PAC3 homodimerization in vitro. PAC3 is the assembly factor of the 20S proteasome and is essential for proteasome activity. The proteasome inhibitor bortezomib has been used as a clinical agent for relapsed multiple myeloma and mantle cell lymphoma. Accordingly, **1** could be a useful primary compound for developing anticancer drugs. Bortezomib binds to the catalytic site of the 26S proteasome with high affinity and specificity to inhibit proteasome activity. In contrast, a different mode-of-action mechanism for proteasome inhibitory activity is expected, because the target site of **1** is the PPI of the PAC3 homodimer. Moreover, compound **1** provides a valuable tool for studying the mechanism of proteasome assembly.

Experimental Section

General Experimental Procedures. Optical rotations were recorded on a SEPA-300 polarimeter (Horiba) and HRESIMS data on an LCT-Premier XE mass spectrometer (Waters). UV and IR spectra were measured on a DU730 UV/vis spectrophotometer (Beckman Coulter) and an FT-720 spectrophotometer (Horiba), respectively. NMR spectra were recorded on an NMR System 600 NB CL (Varian) in acetone-d_6 with the residual solvent peak as an internal standard (δ_C 29.8, δ_H 2.04 ppm) or CDCl$_3$ (δ_C 77.0, δ_H 7.25 ppm). MPLC was done on a Purif-Pack ODS-100 column (Moritex, Tokyo, Japan), analytical HPLC using an L-column2 ODS column (4.6 mm i.d. × 150 mm; Chemical Evaluation and Research Institute, Tokyo, Japan) with a 2996 photodiode array detector (Waters) and a 3100 mass detector (Waters), and preparative RP-HPLC using an L-column2 ODS (20 mm i.d. × 150 mm) or an X-bridge ODS column (19 mm i.d. × 150 mm; Waters). Reagents and solvents of the highest available grade were used.

Strain and Fermentation. *Verticillium* sp. f21794 was isolated from a soil sample collected in Shirakurakyo, Shizuoka Prefecture, Japan, with the daunomycin method developed by Sugimoto et al.[9] The strain was cultured on a rotary shaker (220 rpm) at 25 °C for 4 days in a 500 mL Erlenmeyer flask containing 60 mL of a medium consisting of 2% potato starch, 1% glucose, 2% soybean meal, 0.1% KH$_2$PO$_4$, and 0.05% MgSO$_4$·7H$_2$O.
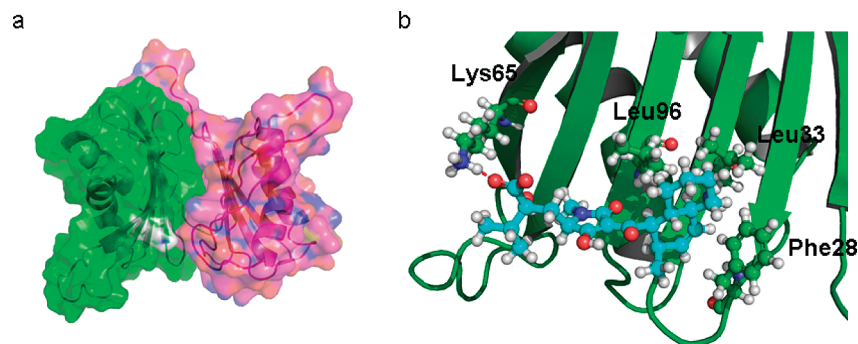
Figure 3. Proposed model for **1** binding to PAC3 homodimer interface from docking study. (a) Structure of PAC3 homodimer (cartoon and surface model). (b) A detail of view of key residues (ball and stick model with green carbon atoms) around **1** (ball and stick model with cyan carbon atoms).

Isolation of 1. The culture broth (30 flasks) was extracted with *n*-butanol. After concentration in vacuo, the dried residue (2.0 g) was chromatographed by RP-MPLC with an H_2O/MeOH linear gradient system (0−100% MeOH), and fractions containing active metabolites were collected. The eluate (70−80% MeOH, 124 mg) was subjected to RP-MPLC with 70% aqueous MeOH and fractions containing active metabolites were collected. The active fraction (27 mg) was subjected to preparative RP-HPLC using an L-column2 ODS column (20 mm i.d. × 150 mm) developed with 85% aqueous MeOH containing 0.075% HCO_2H (flow rate: 10 mL/min) to yield an active metabolite (7.7 mg; t_R = 12.7 min). The active metabolite was subjected to a preparative RP-HPLC using an X-bridge ODS column (19 mm i.d. × 150 mm) developed with 40% aqueous MeCN containing 0.3% Et_2NH (flow rate: 10 mL/min) to yield JBIR-22 (**1**, 4.8 mg; t_R = 15.8 min).

JBIR-22 (1). Colorless amorphous solid; $[\alpha]^{25}_D$ −330 (*c* 0.7, MeOH); UV (MeOH) λ_{max} (log ε) 234 (8.90), 280 (9.24) nm; IR (KBr) ν_{max} 3240, 1720, 1660, 1620 cm^{-1}; ^1H NMR (600 MHz, acetone-d_6) and ^{13}C NMR (150 MHz, acetone-d_6), see Table 1. HRESIMS *m/z* 420.2385 $[M + H]^+$ (calcd for $C_{23}H_{33}NO_6$, 420.2386).

Methylation of 1. Compound **1** (2.0 mg) was dissolved in acetone (200 μL), mixed with 0.2 mg of K_2CO_3 and 10 μL of MeI, and stirred at room temperature overnight. The mixture was diluted with MeOH, evaporated in vacuo, and subjected to a preparative RP-HPLC using an L-column2 ODS column (20 mm i.d. × 150 mm) developed with 85% aqueous MeOH containing 0.075% HCO_2H (flow rate: 10 mL/min) to give JBIR-22 methyl ester (**2**, 1.0 mg, t_R = 15.9 min).

Docking Study. Compound **1** was docked into the X-ray structure of PAC3 (PDB code: 2Z5E) using 5.0 (SP mode) (Schrödinger, Portland, OR). Grid box for docking calculation was defined around the small concavity in the PAC3 homodimer interface. Concavity analysis was performed using the SiteFinder module of MOE (Chemical Computing Group Inc., Montreal, Quebec, Canada). Hydrogen-bonding interaction between **1** and PAC3 and their visualization were generated by PyMOL (DeLano Scientific, Palo Alto, CA).

Cytotoxicity Assay. The human cervical carcinoma cell line HeLa was cultured in DMEM medium (Wako Pure Chemical) supplemented with 10% fetal bovine serum (Gibco), penicillin, and streptomycin at 37 °C in a humidified incubator with 5% CO_2. The cytotoxic activity was estimated by a WST-8 [2-(2-methoxy-4-nitrophenyl)-3-(4-nitrophenyl)-5-(2,4-disulfophenyl)-2*H*-tetrazolium, monosodium salt] colorimetric assay. The HeLa cells were incubated on 384-well plates at a density of 0.2×10^3 cells per well in 20 μL of medium for 5 h and then treated the plates with compounds at various concentrations for 120 h. Next, 2 μL of WST-8 reagent solution (Cell Counting Kit; Dojindo, Kumamoto, Japan) was added and the plates were incubated for 30 min at 37 °C in a humidified incubator with 5% CO_2. The absorbance of the formed formazan dye was measured at 450 nm.

Supporting Information Available: ^1H and ^{13}C NMR, DQF-COSY, HSQC, HMBC, and NOESY, and HRMS data. This material is available free of charge via the Internet at http://pubs.acs.org.

References and Notes

(1) Arkin, M. R.; Wells, J. A. *Nat. Rev. Drug Discovery* **2004**, *3*, 301–317.
(2) Wells, J. A.; McClendon, C. L. *Nature* **2007**, *450*, 1001–1009.
(3) Hashimoto, J.; Watanabe, T.; Seki, T.; Karasawa, S.; Izumikawa, M.; Iemura, S.; Natsume, T.; Nomura, N.; Goshima, N.; Miyawaki, A.; Takagi, M.; Shin-Ya, K. *J. Biomol. Screening* **2009**, *14*, 970–979.
(4) Miyawaki, A.; Karasawa, S. *Nat. Chem. Biol.* **2007**, *3*, 598–601.
(5) Ueyama, T.; Kusakabe, T.; Karasawa, S.; Kawasaki, T.; Shimizu, A.; Son, J.; Leto, T. L.; Miyawaki, A.; Saito, N. *J. Immunol.* **2008**, *181*, 629–640.
(6) Hirano, Y.; Hendil, K. B.; Yashiroda, H.; Iemura, S.; Nagane, R.; Hioki, Y.; Natsume, T.; Tanaka, K.; Murata, S. *Nature* **2005**, *437*, 1381–1385.
(7) Hirano, Y.; Hayashi, H.; Iemura, S.; Hendil, K. B.; Niwa, S.; Kishimoto, T.; Kasahara, M.; Natsume, T.; Tanaka, K.; Murata, S. *Mol. Cell* **2006**, *24*, 977–984.
(8) Moore, B. S.; Eustaquio, A. S.; McGlinchey, R. P. *Curr. Opin. Chem. Biol.* **2008**, *12*, 434–440.
(9) Sugimoto, S.; Watanabe, Y.; Isshiki, K. *Biosci., Biotechnol., Biochem.* **2008**, *72*, 2385–2391.
(10) Steyn, P. S.; Wessels, P. L. *Tetrahedron Lett.* **1978**, *19*, 4707–4710.
(11) Stickings, C. E. *Biochem. J.* **1959**, *72*, 332–340.
(12) Kobayashi, H.; Shin-y, K.; Furihata, K.; Hayakawa, Y.; Seto, H. *Tetrahedron Lett.* **2001**, *42*, 4021–4023.
(13) Murata, M.; Matsuoka, S.; Matsumori, N.; Paul, G. K.; Tachibana, K. *J. Am. Chem. Soc.* **1999**, *121*, 870–871.
(14) Park, H. R.; Chijiwa, S.; Furihata, K.; Hayakawa, Y.; Shin-Ya, K. *Org. Lett.* **2007**, *9*, 1457–1460.
(15) Umeda, Y.; Furihata, K.; Sakuda, S.; Nagasawa, H.; Ishigami, K.; Watanabe, H.; Izumikawa, M.; Takagi, M.; Doi, T.; Nakao, Y.; Shin-Ya, K. *Org. Lett.* **2007**, *9*, 4239–4242.
(16) Furihata, K.; Seto, H. *Tetrahedron Lett.* **1999**, *40*, 6271–6275.
(17) Hellwig, V.; Grothe, T.; Mayer-Bartschmid, A.; Endermann, R.; Geschke, F. U.; Henkel, T.; Stadler, M. *J. Antibiot.* **2002**, *55*, 881–892.
(18) Phillips, N. J.; Goodwin, J. T.; Fraiman, A.; Cole, R. J.; Lynn, D. G. *J. Am. Chem. Soc.* **1989**, *111*, 8223–8231.
(19) Vesonder, R. F.; Tjarks, L. W.; Rohwedder, W. K.; Burmeister, H. R.; Laugal, J. A. *J. Antibiot.* **1979**, *32*, 759–761.
(20) Marfori, E. C.; Kajiyama, S.; Fukusaki, E.; Kobayashi, A. *Z. Naturforsch., C: J. Biosci.* **2002**, *57*, 465–470.
(21) Marfori, E. C.; Kajiyama, S. I.; Fukusaki, E. I.; Kobayashi, A. *Phytochemistry* **2003**, *62*, 715–721.
(22) Singh, S. B.; Zink, D. L.; Goetz, M. A.; Dombrowski, A. W.; Polishook, J. D.; Hazuda, D. J. *Tetrahedron Lett.* **1998**, *39*, 2243–2246.
(23) Yashiroda, H.; Mizushima, T.; Okamoto, K.; Kameyama, T.; Hayashi, H.; Kishimoto, T.; Niwa, S.; Kasahara, M.; Kurimoto, E.; Sakata, E.; Takagi, K.; Suzuki, A.; Hirano, Y.; Murata, S.; Kato, K.; Yamane, T.; Tanaka, K. *Nat. Struct. Mol. Biol.* **2008**, *15*, 228–236.